OXFORD UNIVERSITY PRESS | Environmental Entomology

A Temperature-Dependent Phenology Model for the Sweetpotato Whitefly Bemisia tabaci MEAM1 (Hemiptera: Aleyrodidae)

Journal:	*Environmental Entomology*
Manuscript ID	ENVENT-2022-0213
Manuscript Type:	Research
Date Submitted by the Author:	15-Dec-2022
Complete List of Authors:	Sporleder, Marc; International Potato Center, Crop and System Science Division Gamarra, Heidy; International Potato Center, Crop and System Science Division Carhuapoma, Pablo; Centro Internacional de la Papa, Crop and Systems Sciences Division Goicochea, Luis; National Agrarian University La Molina, Entomology Kroschel, Jürgen; University of Hohenheim Hans-Ruthenberg-Institut, Hans-Ruthenberg Institute Kreuze, Jan; International Potato Center, Crop and Systems Sciences Division
Please choose a section from the list:	Physiological Ecology
Organism Keywords:	Aleyrodidae
Field Keywords:	Population Modeling, Invasive Species, Population Ecology, Thermal Biology, Vegetable Crop Pests

Environmental Entomology

Section: Population Ecology

Article Type: Research

Corresponding Author Name and Address

Marc Sporleder

International Potato Center (CIP)

E-mail: marc.sporleder@aol.de

Short title:

Temperature-dependent phenology of the sweetpotato whitefly

Type of manuscript: Original contribution

A Temperature-Dependent Phenology Model for the Sweetpotato Whitefly *Bemisia tabaci* MEAM1 (Hemiptera: Aleyrodidae)

MARC SPORLEDER[1], HEIDY GAMARRA[1], PABLO CARHUAPOMA[1], LUIS GOICOCHEA[2], JÜRGEN KROSCHEL[3] and JAN KREUZE[1]

[1] Crop and Systems Sciences Division, International Potato Center (CIP), Av. La Molina 1895, Lima 12, Peru International Potato Center (CIP), Apartado 1558, Lima 12, Peru

[2] National Agricultural University La Molina (UNALM), Av. La Molina 15024, La Molina, Lima, Peru

[3] Hans Ruthenberg Institute, University of Hohenheim, Germany

Abstract

The sweetpotato whitefly *Bemisia tabaci* (Gennadius) MEAM1 (Hemiptera: Aleyrodidae) is widely distributed in tropical and subtropical regions affecting more than 600 different species of cultivated and wild plants. Due to the large number of viruses it can transmit, the species is one of the most important economic insect pests in the world. Determination of the pest's temperature-dependent population growth potential is crucial knowledge for understanding the population dynamics and spread potential of the species and the diseases it can transmit, as well as for designing effective pest management strategies. *B. tabaci* MEAM1 development, mortality and reproduction were studied at seven constant temperatures in the range from 12° to 35°C. The Insect Life Cycle Modeling (ILCYM) software was used to fit nonlinear equations to the data and establish an overall phenology model to simulate life-table parameters based on temperature. Life tables of *B. tabaci* MEAM1 established at naturally fluctuating temperature in La Molina, Lima, during different seasons, covering the entire temperature range of the species' predicted performance curve, were used to validate the model. The overall model predicted population development within the temperature range of 13.9° to 33.4°C with a maximum finite rate of population increase (λ=1.138) at 26.4°C. The model gave good predictions when compared with observed life tables and published data. The established process-based physiological model presented here for *B. tabaci* MEAM1 can be used predicting the species distribution potential based on temperature worldwide and should prove helpful in adjusting pest management measures.

Key words: whiteflies, modeling, temperature-dependent development, development rate models, life-table statistics, invasive pests

Introduction

The sweetpotato whitefly *Bemisia tabaci* Middle East-Asia Minor 1 (MEAM1) (Hemiptera: Aleyrodidae), previously known as *B. tabaci* biotype B (formerly also referred to as *B. argentifolii* Bellows & Perring), is an economically important invasive species in many regions of the world causing considerable damages to agriculture crops through direct feeding and indirect vectoring of plant pathogens. The species is a member of the sweetpotato whitefly complex, *Bemisia tabaci* Gennadius, which is described as a complex of cryptic species representing at least 46 morphologically indistinguishable but reproductively isolated groups (Dingsdale et al. 2010, Barro et al. 2011, Rehman et al. 2021, Elfekih et al. 2018). Of these, the groups originating in the Middle-East Asia-Minor (MEAM1), and Mediterranean (MED) regions, are globally invasive pests of hundreds of crop plant species (Oliveira et al. 2001), vectoring over 100 different plant viruses (Jones 2003). The ability to develop resistance to major insecticide classes (in conjunction with its polyphagy) creates a serious challenge to farmers and pest control specialists (Horowitz et al. 2020).

The exact origin of the species is not fully known; however, some studies suggest that the species is native to Pakistan, where the greatest diversity of the species' parasitoids has been found, a criterion considered as a good indication for a genus epicenter (Brown et al. 1995). MEAM1 was first identified in the mid-1980s when it invaded the southern states of North America, displacing an earlier known milder species of *B. tabaci* (referred to as biotype A), across the southwestern United States and Mexico. In the 1990s, MEAM1 further expanded its range including Central and South America and the Caribbean. Today, the species occurs worldwide as primary pest of many fruit, vegetable and ornamental crops in tropical, subtropical,

and less predominantly in temperate regions, being reported from more than 90 countries (CABI 2020). In Peru, the pest was reported for the first time in 1993 in the Rímac, Lurín and Cañete valleys infesting cotton, string beans, and sweetpotato (Rodriguez and Redolfi 1992). In 2000, *B. tabaci* MEAM1 displaced the greenhouse whitefly *Trialeurodes vaporariorum* Westwood (Hemiptera: Aleyrodidae) as the dominant whitefly pest in the Ica valley. Today, it is assumed that *B. tabaci* MEAM1 is widely distributed in most of the coastal valleys in Peru, being the most aggressive whitefly species. The main concern with the whitefly is the species ability to transmit viruses, such as those belonging to the *Begomovirus* (Geminiviridae), *Crinivirus* (Closteroviridae), *Ipomovirus* (Potyviridae), *Torradovirus* (Secoviridae) and some *Carlavirus* (Betaflexiviridae) genera. Climate change might alter the distribution of this pest and increase the risk carrying virus diseases to regions where these were absent previously.

Temperature is one of the most important factors affecting development in ectothermic organisms, explained by temperature's direct effects on enzymatic activities in insects (Schoolfield et al. 1981), and also strongly influences survival and reproduction rates in insects (Bale et al. 2002). Any study of insect populations and in particular one that deals with an agricultural pest aiming in establishing a pest management program, requires an exact determination of these basic pest population (autecological) parameters, that is, development time, survival, fecundity, and sex ratio (Zamani et al., 2006). Detailed knowledge on temperature effects on these parameters in herbivore insect pests can serve as a basis for constructing life tables and for model development. Thus, with precise knowledge of these parameters, the growth potential of a pest population under different temperature conditions, the range where the pest might develop, and seasonal dynamics can be estimated.

Although the biology and ecology of *B. tabaci* MEAM1 have been extensively studied in both field (Quintela et al. 2016, Yee and Toscano 1996) and laboratory (Wagner 1995, Wang and Tsai 1996, Kakimoto et al. 2007, for further merits on earlier studies see references cited in Gerling et al. 1986), the biology (autecological parameters) of *B. tabaci* is affected by host plants (Kakimoto et al. 2007) and may differ in different countries or regions due to genetic and phenotypic plasticity.

The objective of this study was to determine the nonlinear relationship between temperature and development, survival, and fecundity, in the Peruvian *B. tabaci* MEAM1 population through constant temperature experiments, and establish an overall temperature-driven phenology model that provides means for predicting the potential increase rates of field populations in different ecologies zones in Peru. We verified the model using life table data obtained at naturally fluctuating temperatures in La Molina, Peru. Model building and simulations were achieved using the Insect Life Cycle Modeling (ILCYM) software developed by the International Potato Center, Lima, Peru (Sporleder et al. 2013, 2017). Finally, we discuss the modeling outputs compared with results from other studies. The present study is part of the effort to establish phenology models for major insect pests of potato and sweetpotato (Kroschel et al. 2016).

Materials and Methods

Insect origin and mass rearing

A colony of *B. tabaci* MEAM1 was initiated with puparia collected from sweetpotato, *Ipomoea batatas* (Convulvaceae), plantings in La Molina, Lima, Peru. The identity of the population was confirmed by using random amplified polymorphic DNA-polymerase chain reaction (RAPD-PCR. The colony was maintained and mass-reared in the greenhouse at 18°-23°C, 80% relative humidity (RH) and a photoperiod of 12:12 h light (L): dark (D). Field-collected, whitefly-infested sweetpotato leaves were place with their petioles on a sponge soaked in water placed on a tray to ensure that the leaves were hydrated until adult whiteflies emerged. Adults were maintained individually on sweetpotato (cv. Costanero) in insect-proof cages containing two sleeves for in-situ manipulation. For providing oviposition medium, four new sweetpotato plants were placed inside the cage and replaced after a period of five days. After the third whitefly generation, collected adults were used to initiate temperature experiments.

Experimental procedures for data collection

The effects of temperature on the biology of *B. tabaci* MEAM1 were studied in life tables experiments initiated with a number of 100 new-laid eggs and incubated in controlled incubation chambers at seven constant temperatures of 12°, 15°, 18°, 20°, 25°, 32°, and 35°C (Table 1). The temperature and RH inside the incubation chambers were monitored using indoor data loggers (Hobo H8, Onset, MA). RH in the chambers was maintained above 80% and the photoperiod regime was kept at 12:12 h L:D.

Each life table was established as follows:

Five vigorous and uniformly developed potted two-leaf sweetpotato seedlings (cv. Costanero) were covered individually with a 1 L plastic cup (∅ 12 cm). The plastic cups were modified cutting a hole (∅ 6.5 cm) into the lower part, which was replaced with fine muslin (0.1 μm) for ventilation. To initiate a life table temperature experiment, a number of 50 whitefly adults was collected from the insect rearing cage using an insect aspirator (BioQuip Products, CA) and transferred to a two-leaf sweetpotato plant in a plant pot sealed with muslin (henceforth referred to as mini-cage). The mini-cages were incubated for 24-h period in a temperature-controlled chamber at the required constant temperature to allow adult females to lay eggs onto the plants. After the 24 h-oviposition period, all whiteflies were removed from the mini-cages using an aspirator (BioQuip Products, CA). Oviposited *B. tabaci* MEAM1 eggs on the plants were identified using a stereoscope and the position of 10 eggs on each leaf marked using a waterproof marker. Excess eggs were removed using a style. Thus, each mini-cage contained a number of 20 eggs. The mini-cages were labeled, sealed, and incubated at the respective temperature. In each temperature, a number of 5 mini-cages (considered as pseudo-replications) were tested.

The development and survival of each test insect were observed daily during the egg stage and nymph instars, until the test insect reached puparium (also referred to as the 4^{th} instar nymph). Each day newly developed puparia were transferred individually to small petri dishes that remained in the incubation chamber of the required temperature and were subsequently evaluated daily until adult emergence. For assessing adult survival time and daily fecundity of females, emerging adults were sexed and released individually into a mini-cage, which was incubated at the corresponding temperature. During the daily evaluation process, the females were

temporarily transferred to a new mini-cage for easier assessment of the number of eggs laid during the past 24-h period; eggs on the exposed plants were counted using a stereoscope and marked to differentiate them from the new eggs laid the following day. Thereafter, the female was retransferred to the original mini-cage and returned to the incubation chamber. This evaluation was repeated daily until all females died.

Data for model validation

Three life tables of *B. tabaci* MEAM1 were established at naturally fluctuating temperatures in a screen house at the experimental station of CIP in La Molina, Lima (12° 05' S, 76° 57' W, 250 m.a.s.l.) between May 2011 and February 2012. The life tables, each initiated with 100 eggs, were established sequentially—representing winter, spring, and summer condition—using the method described above. Ambient temperature and relative humidity was measured using a data logger (HOBO, Onset, MA) placed near the mini-cages recording data at 1-h intervals throughout the experiments.

Data analysis and modeling

The data were analyzed and the phenology model developed using the Insect Life Cycle Modeling (ILCYM) software Version 4.0 developed by CIP (Sporleder et al. 2017). The ILCYM software uses R-statistics (R Core Team 2018) for all statistical calculations and is freely available from the institute's website https://ilcym.cipotato.org (Sporleder et al. 2017). All data collected (life tables established at the seven constant temperatures for building the model and the three life tables established at fluctuating temperature for validating the model) are available

171 as complementary material on the same webpage. Since the statistical methods used for model
172 building and validation are described elsewhere (manual for Version 4, Sporleder et al. 2017,
173 2013) these are described here in brief only (for further merit on published modeling research
174 using ILCYM see: Sporleder et al. 2016, Mujica et al. 2017, Gamarra et al. 2020b, Aregbesola et
175 al. 2020).
176
177 The software extracted the development time of the different immature life stages, adult
178 longevity, and oviposition time from the life table data, transformed these into censored time-to-
179 event data, and submitted the data to survival analysis. Parametric accelerated failure time (AFT)
180 models (Kalbfleisch and Prentice 2002) were adjusted to the data using the survreg procedure of
181 the survival package in R statistics (Therneau 2020, Therneau and Grambsch 2000). The AFT
182 model uses the logarithm of survival time as the response variable and includes an error term that
183 is assumed to follow a particular distribution. The log-linear representation of the AFT model is:

184 $$ln\, T_i = \mu + \beta_1 x_{1i} + \ldots + \beta_p x_{pi} + \sigma\varepsilon_i \qquad \text{(eq. 1)}$$

185 where lnT_i is the log-transformed survival time of the i^{th} individual, $x_1 \ldots x_p$ are explanatory
186 variables with coefficients $\beta_1 \ldots \beta_p$, ε_i represents residual or unexplained variation in the log-
187 transformed survival times, while μ and σ are intercept and scale parameters, respectively. The
188 lognormal, log-logistic, and Weibull distributions were tested as distribution function, because
189 these log-distributions are in line with Curry's 'oneshape' theory (Curry et al. 1978); that is, the
190 shape parameter of the stage-specific error distribution is assumed to be in relative relation to the
191 median development time—in other words, normalized distributions are expected to have the
192 same shape. Thus, the AFT models provided parameters for determining expected median times
193 and the distributions of the stage-specific development times.

The AFT models were tested at two levels of complexity, using (*i*) temperature (simpler model) and (*ii*) insect batches (mini-cage, replication per temperature, complex model) as explanatory variables. The expected median development times (in days) were calculated from the coefficient estimates associated with temperature x_i (or with insect batch x_i in the complex model), that is for X_1:

$$time\ (X_1) = exp(\hat{\mu} + \hat{\beta}_1) \quad \text{(eq. 2)}$$

Data on female and male adults (senescence time) and oviposition time were pooled including a further categorical additive covariate (either F = female, M = male, O = oviposition) into the model. These models were tested at different levels of complexity; that is, (*i*) individual coefficients, $\beta_{ij,}$ were estimated for each temperature, *i*, and additional covariate, *j*, female, male, and oviposition (complex model), and (*ii*) coefficients, β_i were estimated for each temperature, *i*, and an additional term $\beta_j x_j$ was included in the model for each categorical covariate, *j*. An initial step in fitting an AFT model is determining which distribution should be specified for the survival times T_i. The distribution chosen for T_i prescribes the distribution of the error term ε_i. For instance, if survival times are modeled as a Weibull distribution, the error term is assumed to follow an extreme-value distribution. Likewise, if survival times are modeled using the log-logistic or log-normal distribution, the ε_i are assumed to be logistic or normal, respectively. For each comparison, preliminary models were fit in which the T_i were modeled using the Weibull, log-logistic and log-normal distributions, and the appropriate distribution was selected as the one which minimized the Akaike's Information Criterion (AIC) (Akaike 1973). Final AFT models of different complexities were evaluated based upon likelihood ratio test (against "intercept only" model).

217

218 The *ln* median times until occurrence of the events were calculated for each temperature from the
219 AFT models and subjected to nonlinear regression analysis (using the nls procedure; R statistics).
220 ILCYM provides several different models that are adequate for describing the relationship
221 between temperature and median development time, mortality, adult senescence and oviposition
222 time, and average fecundity per female. For example, >20 models that might describe
223 temperature-dependent development in insects were available and tested (see the list of models
224 in the user manual for ILCYM 4.0). These functions generally are fitted in term of rates
225 (1/median time); however, in ILCYM and in this study the functions were fitted in terms of *ln*-
226 times to address increasing variances with increasing median development times (homogeneous
227 variances across all groups are expected when median times are *ln*-transformed). Survivorship in
228 immature life stages was calculated from the relative frequency of surviving test insects.
229 Different nonlinear models (remodeled quadratic functions) available in the ILCYM package
230 were fitted by regression to describe the mortality ratios in each life stage and fecundity by
231 temperature. Since the data on mortality were count data, GLM regression with Poisson
232 distribution was used to fit the models. Fecundity data were *ln*-transformed prior regression to
233 equalize residual variances across tested temperatures verified by Levene's test. The most
234 appropriate model for describing the temperature effect on any of the above parameters was
235 chosen by comparing Akaike's Information Criterion (AIC) (Akaike 1973) and the corrected
236 AIC (AIC_c) (Hurvich and Tsai 1989), which panelizes stronger extra parameters in the model. In
237 addition, data on fecundity per female were submitted to ANOVA and counts of males and
238 females were analyzed by a Chi-square test for verifying temperature effects on fecundity per
239 female and female ratios.

After all required submodels were established, the "model builder" implemented in the ILCYM software generated an overall temperature-driven phenology model for the species in R code that can be further deployed in a variety of simulations. For validating the established model, life tables consisting of 100 individuals were simulated stochastically using the respective temperature records measured during the course of the validation experiments (age-stage life tables established at ambient fluctuating temperature). The software uses a cohort up-dating algorithm on a 1-day interval, whereby intraday temperature-drive processes were simulated in a 1-h discrete time interval to account for intraday temperature fluctuations. In each 1-day interval the parameters were calculated as follows:

The probability of development from one life stage to the next stage was calculated using the stage-specific temperature-dependent development rate function (see Table 2) in conjunction with the selected distribution and scale parameter in the AFT model (see Table 1). For example, if the log-logistic distribution was selected, the development probability is calculated as:

$$development\ probability = 1 - \left(\frac{1}{\left[1 + \sum_{k=0}^{n} r(T)^{\alpha}\right]}\right) \qquad \text{(eq. 3)}$$

where $\sum_{k=0}^{n} \boldsymbol{r}(\boldsymbol{T})$ is the accumulated development rate (=normalized age) of individuals over the period from stage initialization (k=0) to the nth day depending on temperature, T, and α is the stage-specific shape parameter, which is the inverse of the scale parameter, δ, in the AFT model. Stage-specific daily survival probabilities were calculated using the formula:

$$survival\ probability = (1 - m_i)^{r(T)} \qquad \text{(eq. 4)}$$

where m_i is temperature-dependent mortality in stage i using the established mortality functions (Table 3) and $r(T)$ is the stage-specific temperature-dependent development rate calculated as in

263 eq. 3. This formula assumes that the stage-specific daily survival rate, l_x, is temperature-
264 dependent but unique across all age classes; that is, it assumes the exponential hazard rate
265 function. The female rate was determined as observed in experiments (female rate = number of
266 females/number of males and females).
267
268 For each individual used in the simulation, a random number is generated for development from
269 one stage to the next, survival within each stage, sex, and reproduction. During simulation, when
270 the stage-specific random number for development exceeded the expected age-specific
271 development probability, the individual developed to the next stage. Individuals for which the
272 random number for survival exceeded the expected survival probability were considered as
273 deceased. For individuals reaching adult stage, a random number below the expected female
274 ratio simulated a female, otherwise a male. For females, daily fecundity was calculated using the
275 formula:

276 $$daily\ fecundity\ per\ female = (P_i - P_{i-1}) \times F(T)\varepsilon \qquad \text{(eq. 5)}$$

277 where P_i is the accumulated proportion of eggs laid by a female depending on age. For the
278 Weibull link function, P_i was calculated by:

279 $$P_i = 1 - exp\left(-exp\left(ln\left(\sum_{k=0}^{n} r(T) \times exp(1) \right) \times \alpha \right) \times exp(-\alpha) \right)$$

280 where $\sum_{k=0}^{n} \boldsymbol{r}(\boldsymbol{T})$ is the accumulated oviposition time^{-1} (see function in Table 5) over the period
281 from adult emergence to the *n*th day depending on temperature, T, and α is $1/\delta$, where δ is the
282 scale parameter of the specific Weibull distribution link function (Table 4); and $F(T)\varepsilon$ is the
283 calculated total temperature-dependent fecundity per female using the established model (Table
284 4) and its error distribution (the error distribution was expected to be normal on ln-total

fecundity, a random number was generated that determines the fecundity simulated for each female). For each validation experiment, the simulation was repeated four times.

Differences in development times, mortality rates, oviposition periods, fecundity per female, and resulting life table parameters—namely the net reproduction rate (R_0), mean generation time (T), intrinsic rate of natural increase (r_m), finite rate of increase (λ), and doubling time (Dt) between simulated and observed life tables were statistically evaluated by using z-scores [eq. 6] and t-statistics

$$z = \frac{observed\ value - simulated\ value}{standard\ deviation\ of\ the\ simulated\ value} \quad \text{[eq. 6]}$$

After model validation, life table parameters for *B. tabaci* MEAM1 were simulated from the established model over a range of constant temperatures according to Maia et al. (2000) by using the approximate method (approximate estimate for T). For further detail on the algorithms employed in ILCYM software we refer to Sporleder et al. (2016, 2017).

Results

Development and its distribution

The variation in development times among individuals in the immature life stages across all temperatures was best described in all immature life-stages, egg, 1st to 3rd instar nymph, and puparium (4th instar nymph), by using a log-logistic distribution link function in the accelerated failure time (AFT) models (Table 1). For each life stage, the AFT models revealed highly significant common scale parameters, thus satisfactorily describing the temperature-independent variability in development times among individuals, and temperature-depending coefficients ($P < 0.001$), revealing a significant effect of temperature on the development times (likelihood ratio

test: in all stages $P < 0.001$). Expected median development times resulting from the coefficients of the AFT model decreased significantly with increasing temperature (Table 1). The simpler models provided as good as fit for the data as the complex model (with coefficients for each group tested in a mini-cage; likelihood ratio test: in all stages $P > 0.99$), indicating that the variation in development among groups within each temperature was small. Because all test insects died at 12° and 35°C during nymph stage, the development times in nymphs and puparia could not be determined at these temperatures.

The relationships between temperature and median developmental rates in all three evaluated immature life stages, egg, nymph (N_1-N_3), and puparium were, among several statistically good-fitting models, best described by a Janisch model (Fig. 1, Table 2). The models explained >97% of the variation in median development times by temperature in each stage. The fastest development, estimated by the parameter T_{opt} in the Janisch model, was at temperatures of about 30°, 26° and 33°C for egg, nymph, and puparium stages, respectively.

Immature Mortality

The effect of temperature on the mortality of *B. tabaci* MEAN1 immature stages (Table 1) was best described by the following nonlinear model (Table 3; Fig. 2).

$$logit\, m_i(T) = logit\, m_{min} + \alpha(T_{opt} - T)^2 \qquad \text{[eq. 7]}$$

$$m_i(T) = \frac{\exp\,(logit\, m_i(T))}{1 - \exp\,(logit\, m_i(T))}$$

where $logit\, m_i(T)$ is the logit-transform of the overall percent mortality, $m_i(T)$, in life stage i, depending on temperature T, $logit\, m_{min}$ is the logit-transform of the minimum percent mortality at optimum temperature, T_{opt}, in °C, and α is a shape parameter that determines the increase in

mortality as temperature deviates from the optimum temperature. This model estimated the optimum temperature for survival at 23.8°, 24.3°, and 24.8°C in eggs, nymphs, and puparium, respectively (Table 3). Within the optimal range of temperature expected mortality ratios were <8% in all life stages. Mortality increased severely (>50%) at temperatures <13.3° and >34°C in eggs, <15° and >33.3°C in nymphs, and <11.3° and >41.3°C in puparia (Fig. 2).

Adult lifespan and fecundity

The variation in adult male and female survival times and oviposition periods among individuals across all temperatures was best described by using the Weibull distribution in the AFT models. The models revealed significant effects of temperature on adult survival time and females' oviposition time (Table 4). Using an additive factor, λ_{male}, which estimates the difference in the survival time of males compared with females across all temperatures, provided the best fit according to AIC_c for modeling adult lifespan. The estimated value of λ_{male} (Table 4) revealed that the lifespan of males was generally about 12.3% shorter than of females. Adult lifespan showed a parabolic temperature curve with a maximum lifetime at 18°C, with gradually decreasing survival times within the temperature range from 15°C to 25°C (lifetimes did not differ significantly), while at 32°C lifetime decreased significantly.

The AFT model for oviposition time revealed the best fit, according to AIC_c, when individual coefficients were included for females and oviposition at each temperature instead of pooling the data with female lifetime and using a single additional factor, $\lambda_{oviposition}$, which estimates a relative difference in the oviposition period compared to female lifetime across all temperatures. The likelihood-ratio-test between these two models revealed equal fit (P = 0.874), indicating a

strong linear relationship between female lifespan and oviposition period, although the ratio between the two figures was not constant across temperatures. Therefore, the AFT model for oviposition period was adjusted using coefficients for each temperature and a specific scale factor (Table 4).

Fecundity per female was extremely variable, ranging from 5 to 805 eggs per females observed at 25°C (see Table 4). The standard deviations appear strongly related to mean fecundity and, as expected, the variance was not equal over the temperatures tested (Levene's test: $p < 0.001$). A Levene test revealed homogeneous variances across all temperatures after *ln*-transformation of the data ($F = 1.75$, $df = 4, 183$, $P = 0.14$), and ANOVA on *ln*-transformed numbers of eggs produced per female revealed a significant effect of temperature on fecundity ($F = 75.4$, $df = 4, 183$, $P < 0.001$). Group-wise comparison indicated significant differences in fertility between temperatures (see Table 4).

The relationships between temperature and adult median lifespan as well as median oviposition time were significantly described by a nonlinear remodeled quadratic function (see Table 5, Fig. 3a) (due to increasing variances with increasing medians the functions were fitted in terms of *ln*-times). The AIC_c values indicated that the function using generally 12.3% reduced survival time for males (while other parameters remained the same for males and females) was most likely the best model for describing both male and female longevity. Median oviposition time could be significantly described by the same model; however, fitting the function with individual parameters. These models predict symmetric parabolic temperature-curves, indicating longest survival time for females (69.6 days) at an optimum temperature of 19.5°C. Temperature-

dependent total fecundity per female could be described by a Taylor model in which fecundity decreased symmetrically from a maximum of 536 eggs per female at a temperature of 22.6°C to below 20 eggs per female at temperatures <14,1° and >31°C (Fig. 3b, Table 5). The cumulative fecundity frequencies in relation to normalized oviposition time (female age) were modeled by using a Weibull distribution function (Fig 3c).

More females than males were reproduced across all temperatures; however, the female-male ratio was quite variable among the temperatures tested (varied from 3:1 at 32°C to 1.07:1 at 15°C). A chi-square test rejected the hypothesis of equal female ratios across temperature (Chi^2 = 30.75; df = 19; p = 0.043) (Fig. 3d). The female ratio decreased from about 74% at 25°C and above with decreasing temperature to about 52% at 15°C.

Model validation

The compiled model predicted reasonably the autecological parameters derived from the three life tables established at fluctuating temperature in La Molina (Tab. 6, Fig. 4). The daily temperature variations measured during the course of the life table experiments were within the permissive temperature range predicted by the model for the evolution of whitefly populations. Average minimum and maximum temperatures measured during the three life table experiments were *1)* 14.6°C and 21.3°C, respectively (winter), which represents the lower curvilinear temperature range (from the minimum critical temperature, CT_{min}, to the inflection point at which the performance curve switches between accelerating upwards to decelerating upwards) of the species-specific performance curve, *2)* 16.4°C and 26.4°C (Spring), which represents the middle region of the performance curve (linear region up to the temperature at which growth is at

maximum), and *3)* 19.5°C and 29.7°C (summer), which represents upper temperature range of the performance curve (from below the inflection point to behind the optimal temperature, T_{opt}, at which the performance curve switches down to a slowdown in performance), but not reaching the upper limit of performance, CT_{max}.

Convergences between simulated and observed stage-specific development times, mortality rates, adult survival time, fecundity and resulting life-table parameters (according to z-scores) are presented in Tab. 6. The model overestimated slightly but (statistically) significantly immature development times observed in spring (for the total development time about 10%) and summer (about 16%). Mortality in eggs and nymphs was significantly overestimated in spring (the total immature mortality was with about 46% more than double as high as observed), while in all other cases mortality was satisfactorily simulated. Female lifetime, oviposition period, and fecundity per female were quite well predicted; only in winter female lifetime was significantly underestimated (-25%), while oviposition period was significantly overestimated only in spring (+14%). Fecundity per female was perfectly simulated in spring, but about 19% and 52% underestimated in summer and winter, respectively. Although there was a high level of agreement in the life table parameters by using the same female ratio in the simulation as observed in each of the three life tables, population growth potential was generally slightly underestimated (see probabilities according to the z-scores in Tab. 6). The simulated intrinsic rate of increase, for example, deviated relatively -20% (spring), -12% (winter), and -13% (summer) from the intrinsic rate of increase calculated from the observed life tables. The overall conformity of the simulated results with the observed data is demonstrated visually in Fig. 4 by

422 contrasting the simulated and observed age-stage-specific and age-specific survival rates and
423 age-specific fertility.
424
425 *Life table parameters*
426 The model predicted temperature limits for population development (permissive range) from
427 13.8°C to 33.6°C (Fig. 5). Maximum population growth is expected at around 26.3°C with a
428 finite rate of increase, λ, of 1.163 (see Fig. 5a), which corresponds with a population doubling
429 time of 4.6 days. Thermal performance curves at fluctuating temperatures generally flatten as
430 explained by the Kaufmann effect (Worner 1992). For illustrating the Kaufmann effect
431 anticipated by the model, life tables were simulated using a daily temperature cycle of ±5°C.
432 These simulations were carried out in 1-hour intervals using a sine wave function between the
433 daily minimum temperature (average temperature minus 5°C) and maximum temperature
434 (average temperature plus 5°C). These temperature fluctuations flatten the performance curves
435 (see scattered lines in Fig. 5), augmenting the permissive range with thresholds at minimum
436 mean temperature of 12.1 (±5)°C, and maximum mean temperature of 34.9 (±5)°C, with optimal
437 mean temperature of 27.7°C for maximum population growth.
438
439 ## Discussion
440 In the presented study, we examined the effects of temperature on all physiological processes in
441 *B. tabaci* MEAM1 populations over the entire temperature range in which the species is expected
442 to develop. For the parameters studied, namely the development time and survival in pre-adult
443 life stages, and longevity, fecundity and female ratios in adults, functions describing the
444 dependence on temperature were established and compiled into an overall temperature-based

445 (phenology) rate summation model. This model allows simulating life table parameters and thus
446 population growth potentials for different ecological regions and seasonal climatic variations.
447 Such knowledge on pest's population growth is essentially for designing pest management
448 strategies taking into account population development in different agroecosystems.
449
450 Comprehensive research has been conducted on studying the effect of temperature on *B. tabaci*
451 MEAM1 in different crops. We compared our findings with literature results reported from
452 constant temperature experiments for *B. tabaci* MEAM1 on different host plants (limited to
453 reports) published after the year 1995, namely Yang and Chi (2006) [using tomato as host crop],
454 Qui et al. (2003) [eggplant], Wang and Tsai (1996) [eggplant], Nava-Camberos et al. (2001)
455 [cotton, sweet melon], Muniz and Nombela (2001) [sweet pepper], Wagner (1996) [cotton], and
456 Kakimoto et al. (2007) [eggplant, cucumber, sweet pepper, tomato], since earlier studies refer to
457 *Bemisia tabaci* sensu lato, where it could not be verified which species were studied (for further
458 merits of earlier publications on this topic see the review by: Gerling et al. 1986).
459
460 Based our constant temperature experiments, the established (Janisch) models for describing
461 temperature-dependent development in eggs, nymphs (instars N_1-N_3) and puparia (N_4) largely
462 agree with the findings of other researchers. For example, reported development times in
463 whitefly eggs were similar, following the same trend, as modeled in this study. The development
464 time gradually decreased with increasing temperature from 12°C (41 days) to a minimum at
465 30°C (4.1 days), and increased again with increasing temperature above 30°C (about 5.6 days at
466 35°C). For visual comparison, the development times reported in the literature were transformed
467 into rates and plotted against temperature together with the observed data and predictions of this

study (see Figure 6a). A direct comparison of the development times of nymphs and pupae was difficult, because in other studies either individual nymphal instars—with the transition to the puparium (N_4) had been determined differently—or all stages together were examined. However, comparing the total development times from egg to adult reported in the literature with the results and predictions of this study reveals a high level of agreement (see Figure 6b); showing slightly overestimated development times in the lower temperature range between 15° and 20°C, and convergence at higher temperatures, including predicting the shortest pre-adult development time (16.5 days) at about 28°C. At temperatures above 30°C development times from other studies varied increasingly. Although adaptation to a particular host plant might affect development times in a population, the high variability in development at high temperature suggests that local populations have adapted differently to higher temperatures and altered their tolerance to heat stress. Therefore, the shorter development time observed in this study below 20°C and above 30°C could be a specific characteristic of the whitefly population prevailing on sweetpotato in Peru.

Mortality rates in immature life stage reported in the literature were quite variable. Egg viability in other studies was generally higher (>90%) than in this study (see Fig. 6c), while data reported on the mortality in nymphs, particularly in the first three nymphal instars and less in puparium, showed extreme variability. However, the temperature-dependent mortality curves established in this study, indicating significantly increased mortality at temperatures below 15°C and above 35°C in all immature life stages, and hence the overall predicted percentage survival from egg to adult across temperatures in this study was supported by most literature data (see Figure 6d). Lowest mortalities were observed by Nava-Camberos et al. (2001) on sweet melon, while the

491 highest mortalities were observed by the same authors on cotton and by Qiu et al. (2003) on
492 eggplant. This suggests that mortality, particularly in the first three nymphal instars, is strongly
493 determined by host plants and the degree of adaptation of a given whitefly population to its
494 primary host crop.
495
496 In this study, adult survival time of the whitefly was generally longer (and fecundity higher) than
497 reported from other studies; with the relative differences being variable over the temperature
498 range tested (Fig. 6e). Shortest adult survival time was observed by Yang and Chi (2006) in
499 rearing the whitefly on tomato in Taiwan. At temperatures between 20° and 30°C adult lifespan
500 was about 15 days, thus about 4-times shorter than observed in this study. Of the literature data
501 used, only Yang and Chi (2006) reported adult survival time at 15°C, where the discrepancy in
502 lifespan was quite huge; about 5.5 and 50 days observed by Yang and Chi (2006) and in this
503 study, respectively. It seems that the Taiwan whitefly population reared on tomato already
504 responded to cold temperature inhibition at 15°C, while the Peruvian population reared on
505 sweetpotato still tolerates such temperature. Although adult life expectancy predicted in this
506 study suggests progressively shorter survival times with temperatures falling <15°C (see Fig.
507 6e).
508
509 At temperatures <30°C, lifetime fecundity observed in this study was higher than in any of the
510 other studies mentioned above (Fig. 6f). The predicted temperature-dependent fecundity in this
511 study closely corresponds with the findings by Wang and Tsai (1996) for a Florida population of
512 the whitefly reared on eggplant. Kakimoto et al. (2007) showed that fecundity per female is
513 highly variable when *B. tabaci* MEAM1 (Japanese population) is reared on different host plants;

514 whiteflies reared on eggplant, from which the population was originally collected, produced
515 highest fecundity followed by cucumber, sweet pepper and tomato. Similarly, Tsai and Wang
516 (1996) reported highest fecundity and female longevity for the Florida population on eggplant,
517 followed by tomato, sweetpotato, garden bean, and cucumber (see Fig. 6f). The Florida
518 population was established from whiteflies collected from eggplants. While at 25°C the female
519 lifespan was 24 days and fecundity 224 eggs per female when reared on eggplant, this reduced to
520 16.6 days and 77.5 eggs per female when reared on sweetpotatoes. For comparison, the lifespan
521 of females in this study was 51 days and 369 eggs were laid per female. This shows how
522 significantly the potential reproductive performance, and consequently population development,
523 depends on the preferred host plant to which the population has adapted.
524
525 Our observation of an imbalanced sex ratio in favor of females in whiteflies completing
526 development largely agrees with the findings of other researchers. Wagner (1995) observed a
527 female to male ratio of almost 2:1; however, in his experiment, temperature did not affect the
528 proportion of females (determined by regression; slope was not significantly different from
529 zero). Qui et al. (2002) reported female ratios between 1.1 and 1.4 to 1, thereby–in contrast to
530 our results–the female ratio (gradually) decreased as temperature increased but observed
531 difference among different temperature experiments were non-significant. An average female
532 ratio of 1.85:1 was observed by Tsai and Wang (1996) at temperature of 25°C across different
533 host plants. Being arrhenotokous, *B. tabaci* MEAM1 may lay unfertilized eggs that develop into
534 males only. Gerling et al. (1986) revised several earlier field studies on *B. tabaci* and stated that
535 the sex ratio in emerging adults is unstable and that the ratio between fertilized and unfertilized
536 eggs changes with various conditions. That is why we used a sex ratio equal to the sex ratio as

observed in our life table experiments for validating the established model. However, since females are generally more numerous than males, we found it reasonable using the overall female ratio of 0.66% (1.5:1 ♀:♂) for further simulations in the established model.

The insect population growth rate, derived from development times, survival rates, reproduction and sex ratios, is an important estimated demographic parameter used in pest risk assessment. The finite rate of increase, λ, simulated in this study compared to estimates reported in the literature for the whitefly is demonstrated in Fig. 6g. The prediction of the highest rate of increase at about 26°C with $\lambda = 1.1625$ agrees well with reports from other studies. Wang and Tsai (1996) observed maximum rate of increase ($\lambda = 1.211$) at temperature between 25° and 27°C and a drop to $\lambda = 1.076$ at 35°C due to adverse effects of high temperature. Yang and Chi (2006) obtained a maximum intrinsic rate of increase ($\lambda = 1.1907$) at 30°C and Qui et al. (2003) with $\lambda = 1.16$ at 29°C. Guo et al. (2012) studied the effects of high temperature (≥27°C) on life table parameters over five successive generations and observed decreasing rates of increase at temperatures of 31°C and, more evident, at 35°C, in the fourth and fifth generation while at 27°C the finite rate of increase remained high with no significant differences in λ among the five successive generations (λ between 1.124 and 1.128). The inflection point of the expected λ-(performance) curve in this study, where population growth slows down due to adverse high-temperature effects, agrees well with literature data, although the decline in population growth was more pronounced in this study. While at temperature of 35°C other studies revealed a positive population growth rate, in this study the growth rate was already negative (see Fig 6g). Toward lower temperature, the predicted growth rate corresponds well in the mid-range of linear increasing population growth (from about 17° to 23°C; see results from Yang and Chi (2006),

Wang and Tsai (1996) and Qiu et al. (2003) in Fig. 6g). However, at 15°C our model still reveals population increase ($\lambda = 1.012$) while Yang and Chi (2006) reports a negative increase rate.

The established model agrees with most observations that the species was usually able to complete development in the temperature range of 15-35°C, with survival usually being substantially reduced at temperature < 20°C or > 30°C. Ikemoto (2005) elaborated that insect species adapting to a new environment or host plant do not change their intrinsic optimum temperature for development, which is approximately the inflection point of the performance curve, but alter their tolerance to cold and hot temperature. The inflection point determined in this study for development time (at about 23.6°C) and of the predicted λ-(performance) curve converges well with results of other studies. It should be noted that immature survival and fecundity was also at maximum at temperature of about 23.6°C. Therefore, increasing divergences in development performance between the Peruvian whitefly population used in this study and observations on *B. tabaci* MEAM1 studied in other parts of the world as temperature deviates from the inflection point can be attributed to adaptation of the population to the prevailing environment. The established phenology rate model quite well explained the whiteflies life history parameters in contrasting seasonal temperature regimes in La Molina, Peru, and can be applied using daily fluctuating and seasonally oscillating temperatures coping well with the Kaufmann effect (Worner, 1992, Ikemoto and Egami 2013). The Kaufmann effect means that the temperature-growth performance curve flattens with increasing temperature fluctuations when plotted against mean temperatures, making development possible at mean temperatures outside the temperature limits determined from constant temperature experiments (as demonstrated in Fig. 5). This illustrates that the pest might also develop at locations or during

583 seasons in which the mean temperature is below the determined temperature limit. As a further
584 advantage, the approach also allows determining the variances expected in individual
585 development processes.
586
587 Several attempts were made to predict the global species distribution risk for *B. tabaci* MEAM1,
588 particularity in view of climate change based solely on distribution data using different models
589 (Herrera Campo et al. 2011, Kriticos et al. 2020), which resulted in variable or even unreliable
590 distribution projections. The established phenology rate model in this study produced reasonable
591 life table parameters for the whitefly based on temperature and could therefore, if linked to
592 Geographic Information Systems, produce maps that allow predictions of population and
593 distribution changes in response to changing temperatures as influenced by global warming.
594 Thus, this model could be used for cross-validating existing species distribution maps established
595 using distribution data.
596
597 In conclusion, the simulated life table parameters for *B. tabaci* MEAM1 reflect the temperature-
598 dependent population growth potential of the whitefly population producing reasonable life table
599 parameters for the whitefly based on temperature and could therefore produce maps that allow
600 predictions of population and distribution changes in response to changing temperatures as
601 influenced by global warming. The model should be particular helpful for predicting the
602 potential distribution and geography specific risk assessment of the whitefly attacking
603 sweetpotato across Peru and beyond. Its use for simulating realistic *B. tabaci* MEAM1
604 establishment and spread risk potential in other host crops or other regions should be further
605 evaluated. Further, if MEAM1 *B. tabaci* species might become established in new

areas/countries its polyphagous feeding activities could enable viruses to move into new susceptible host plants, causing new crop protection problems, and this model could be also used for predicting the risk of new plant diseases transmitted by the pest as was demonstrated for the greenhouse whitefly and potato yellow vein virus (Gamarra et al. 2020a).

Acknowledgements

We are thankful to Luz Supanta and Jorge Chavez for support during data collection. The research presented was undertaken as part of and funded by, the CGIAR Research Program on Roots, Tubers and Bananas (RTB) and Plant Health Initiative and supported by CGIAR Fund Donors (https://www.cgiar.org/funders/).

References

Akaike, H. 1973. Information theory as an extension of the maximum likelihood principle, pp. 276–281, In: Petrov, B.N., Csaki, F. (ed.) Second International Symposium on Information Theory. Akademiai Kiado, Budapest.

Aregbesola, O. Z., J. P. Legg, O. S. Lund, L. Sigsgaard, M. Sporleder, P. Carhuapoma, and C. Rapisarda. 2020. Life history and temperature-dependence of cassava-colonising populations of *Bemisia tabaci*. J. Pest Sci. 93 (4): 1225–1241.

Bale J.S., G. J. Masters, I. D. Hodkinson, C. Awmack, T. M. Bezemer, V. K. Brown, J. Butterfield, A. Buse, J. C. Coulson, J. Farrar, J. E. G. Good, R. Harrington, S. Hartley, T. H. Jones, R. L. Lindroth, M. C. Press, I. Symrnioudis, A. D. Watt, and J. B. Whittaker. 2002. Herbivory in global climate change research: direct effects of rising temperature on insect herbivores. Global Change Biol. 8: 1–16.

Barro, P. J. de, S.-S. Liu, L.M. Boykin, and A. B. Dinsdale. 2011. *Bemisia tabaci*: A statement of species status. Annu. Rev. Entomol. 56: 1–19.

Brown, J. K., D. E. Frohlich, and R. C. Rosell 1995. The sweetpotato or silverleaf whiteflies: biotypes of *Bemisia tabaci* or a species complex? Annu. Rev. Entomol. 40(1), 511-534.

CABI. 2021. *Bemisia tabaci* (MEAM1) (silverleaf whitefly). In: Invasive Species Compendium. Wallingford, UK: CAB International. www.cabi.org/isc.

Curry, G. L., R. M. Feldman, and P. J.H. Sharpe. 1978. Foundations of stochastic development. J. Theor. Biol. 74: 397–410.

Dinsdale, A., L. Cook, C. Riginos, Y. M. Buckley, and P. D. Barro. 2010. Refined global analysis of *Bemisia tabaci* (Hemiptera: Sternorrhyncha: Aleyrodoidea: Aleyrodidae) Mitochondrial Cytochrome Oxidase 1 to Identify Species Level Genetic Boundaries. Annu. Entomol. Soc. Am. 103(2): 196–208.

Elfekih, S., P. Etter, W. T. Tay, M. Fumagalli, K. Gordon, E. Johnson, and P. D. Barro. 2018. Genome-wide analyses of the *Bemisia tabaci* species complex reveal contrasting patterns of admixture and complex demographic histories. PloS one 13: e0190555.

Gamarra, H., Carhuapoma, P., Cumapa, L., González, G., Muñoz, J., Sporleder, M. and Kreuze, J., 2020a. A temperature-driven model for potato yellow vein virus transmission efficacy by Trialeurodes vaporariorum (Hemiptera: Aleyrodidae). Virus research, 289, p.198109.

Gamarra, H., M. Sporleder, P. Carhuapoma, J. Kroschel, and J. Kreuze. 2020b. A temperature-dependent phenology model for the greenhouse whitefly *Trialeurodes vaporariorum* (Hemiptera: Aleyrodidae). Virus Research. 289: 198107. https://doi.org/10.1016/j.virusres.2020.198107

652 **Gerling, D., A. R. Horowitz, and J. Baumgaertner. 1986.** Autecology of *Bemisia tabaci*.
653 Agric. Ecosyst. Environ. 17: 5–19.
654 **Herrera Campo, B., G. Hyman, and A. Bellotti. 2011.** Threats to cassava production: known
655 and potential geographic distribution of four key biotic constraints. Food Secur. 3(3): 329–
656 345.
657 **Horowitz, A. R., M. Ghanim, E. Roditakis, R. Nauen, and I. Ishaaya. 2020.** Insecticide
658 resistance and its management in *Bemisia tabaci* species. J. Pest Sci. 93: 893–910.
659 **Hurvich, C.M., and C. L. Tsai. 1989.** Regression and time series model selection in small
660 samples. Biometrika. 76 (2): 297–307.
661 **Ikemoto, T., 2005.** Intrinsic optimum temperature for development of insects and mites. Environ
662 Entomol 34, 1377–1387.
663 **Janisch, E. 1932.** The infuence of temperature on the life history of insects. Trans. Entomol.
664 Soc. Lond., 80: 137-168.
665 **Jones, D. R. 2003.** Plant viruses transmitted by whiteflies. Eur. J. Plant Pathol. 109(3): 195-219.
666 **Kakimoto, K., H. Inoue, T. Yamaguchi, S. Ueda, K.-i. Honda, and E. Yano. 2007.** Host plant
667 effect on development and reproduction of *Bemisia argentifolii* Bellows et Perring (*B. tabaci*
668 [Gennadius] B-biotype) (Homoptera: Aleyrodidae). Appl. Entomol. Zool. 42: 63–70.
669 **Kalbfleisch, J.D., and R. L. Prentice. 2002.** The Statistical Analysis of Failure Time Data, 2nd
670 ed. Wiley Series in Probability and Statistics. John Wiley & Sons, Inc., Hoboken, NJ, USA.
671 **Kriticos, D. J.; P. J. de Barro, T. Yonow, N. Ota, R. W. Sutherst. 2020.** The potential
672 geographical distribution and phenology of *Bemisia tabaci* Middle East/Asia Minor 1,
673 considering irrigation and glasshouse production. Bull. Entomol. Res. 110 (5): 567–576.

Kroschel, J., N. Mujica, P. Carhuapoma, M. Sporleder. 2016. Pest Distribution and Risk Atlas for Africa. Potential global and regional distribution and abundance of agricultural and horticultural pests and associated biocontrol agents under current and future climates. International Potato Center. (URL: https://cipotato.org/riskatlasforafrica/)

Maia, A.D.H., A. J. Luiz, C. Campanhola. 2000. Statistical inference on associated fertility life table parameters using jackknife technique: Computational aspects. J. Econ. Entomol. 93 (2): 511–518.

Mujica N., M. Sporleder, P. Carhuapoma, and J. Kroschel. 2017. A temperature-dependent phenology model for *Liriomyza huidobrensis* (Diptera: Agromyzidae). J. Econ. Entomol. 110(3): 1333–1344.

Muñiz, M., and G. Nombela. 2001. Differential variation in development of the B- and Q-biotypes of *Bemisia tabaci* (Homoptera: Aleyrodidae) on sweet pepper at constant temperatures. Environ Entomol 30: 720–727.

Nava-Camberos, U., D. G. Riley, and M. K. Harris. 2001. Temperature and host plant effects on development, survival, and fecundity of *Bemisia argentifolii* (Homoptera: Aleyrodidae). Environ Entomol 30: 55–63.

Oliveira, M. R. V., T. E. Henneberry, and P. Anderson. 2001. History, current status, and collaborative research projects for *Bemisia tabaci*. Crop Prot. 20(9): 709-723.

Qiu, B. L., S. X. Ren, N. S. Mandour, and L. Li. 2003. Effect of temperature on the development and reproduction of *Bemisia tabaci* B biotype (Homoptera: Aleyrodidae). Insect Science 10: 43–49.

Quintela, E. D., A. G. Abreu, J. F. D. S. Lima, G. M. Mascarin, J. B. D. Santos, and J. K. Brown. 2016. Reproduction of the whitefly *Bemisia tabaci* (Hemiptera: Aleyrodidae) B biotype in maize fields (*Zea mays* L.) in Brazil. Pest. Manage. Sci. 72: 2181–2187.

R Core Team. 2018. R: A language and environment for statistical computing. R Foundation for Statistical computing. (URL: http://www.R-project.org/)

Rehman M., P. Chakraborty, B. Tanti, B. Mandal, and A. Ghosh. 2021. Occurrence of a new cryptic species of *Bemisia tabaci* (*Hemiptera: aleyrodidae*): an updated record of cryptic diversity in India. Phytoparasitica. 49: 869-882.

Rodriguez C., and I. Redolfi. 1992. *Bemisia tabaci* (Homoptera: Aleyrodidae) y sus parasitoides en camote cultivado en la costa central peruana [*Bemisia tabaci* (Homoptera: Aleyrodidae) and its parasitoids in sweet potato cultivated in Peruvian central cost]. Rev. Per. Entomol. 35: 77-81.

Schoolfield, R. M., P. J. H. Sharpe, and C. E. Magnuson. 1981. Non-linear regression of biological temperature-dependent rate models based on absolute reaction-rate theory. J. Theor. Biol. 88: 719–731.

Sporleder, M., P. Carhuapoma, E. Z. H. Tonnang, H. Juarez, H. Gamarra, R. Simon, and J. Kroschel. 2017. ILCYM - Insect Life Cycle Modeling. A software package for developing temperature-based insect phenology models with applications for local, regional and global analysis of insect population and mapping, International Potato Center, Lima, Peru. pp 175. (URL: https://research.cip.cgiar.org/confluence/display/ilcym/Downloads)

Sporleder, M., J. Kroschel, M. R. G. Quispe, A. Lagnaoui. 2004. A temperature-based simulation model for the potato tuberworm, *Phthorimaea operculella* Zeller (Lepidoptera; Gelechiidae). Environ. Entomol. 33(3): 477–486.

718 **Sporleder, M., B. Schaub, G. Aldana, and J. Kroschel. 2016.** Temperature-dependent
719 phenology and growth potential of the Andean potato tuber moth, *Symmetrischema tangolias*
720 (Gyen) (Lep., Gelechiidae). J. Appl. Entomol. 141(3): 201-218.
721 **Sporleder, M., H. E. Z. Tonnang, P. Carhuapoma, J. C. Gonzales, H. Juarez, and J.**
722 **Kroschel. 2013.** Insect Life Cycle Modelling (ILCYM) software - a new tool for regional
723 and global insect pest risk assessments under current and future climate change scenarios, pp.
724 412–427, In: Peña, J.E. (Ed.), Potential Invasive Pests of Agricultural Crops. CABI,
725 Wallingford.
726 **Tsai, J. H., and K. Wang. 1996.** Development and reproduction of *Bemisia argentifolii*
727 (Homoptera: Aleyrodidae) on five host plants. Environ. Entomol. 25(4): 810–816.
728 **Therneau, T. M. 2020.** A Package for Survival Analysis in R. R Package Version 3.1-12.
729 https://CRAN.R-project.org/package=survival.
730 **Therneau, T. M., and P. M. Grambsch. 2000.** Modeling Survival Data: Extending the Cox
731 Model. Springer, New York, ISBN 0-387-98784-3.
732 **Wagner, T.L. 1995.** Temperature-dependent development, mortality, and adult size of
733 sweetpotato ehitefly biotype B (Homoptera: Aleyrodidae) on cotton. Environ. Entomol.
734 24(5): 1179-1188.
735 **Wang, K., and J. H. Tsai. 1996.** Temperature effect on development and reproduction of
736 silverleaf whitefly (Homoptera: Aleyrodidae). Ann. Entomol. Soc. Am. 89: 375–384
737 **Worner, S.P., 1992.** Performance of phenological models under variable temperature regimes:
738 consequences of the Kaufmann or rate summation effect. Environ. Entomol. 21(4): 689–699.
739 **Yang, T.-C., and H. Chi. 2006.** Life tables and development of *Bemisia argentifolii*
740 (Homoptera: Aleyrodidae) at different temperatures. J. Econ. Entomol. 99: 691–698

Yee, W. L., and N. C. Toscano. 1996. Ovipositional preference and development of *Bemisia argentifolii* (Homoptera: Aleyrodidae) in relation to alfalfa. J. Econ. Entomol. 89: 870–876.

Zamani A.A., A.A. Talebi, Y. Fathipour, V. Baniameri. 2006. Effect of temperature on biology and population growth parameters of *Aphis gossypii* Glover (Hom., Aphididae) on greenhouse cucumber. J. Appl. Entomol. 130: 453–460.

Captions:

Table 1. Median development times resulting from accelerated failure time modeling and observed survival rates in the immature *B. tabaci* MEAM1 life-stages at constant temperatures. For the AFT models, the error distributions used, their scales, δ, and the models goodness-of-fit evaluated based upon likelihood ratio test are presented in the lower part of the table.

Table 2. Estimated parameters of the Janisch model fitted to describe temperature-dependent median development rates (1/day) in immature life-stages of *B. tabaci* MEAM1.

Table 3. Estimated parameters of the nonlinear model fitted to describe temperature-dependent mortality in immature life-stages of *B. tabaci* MEAM1.

Table 4. Female survival times, oviposition times (resulting from accelerated failure time modeling) and total fecundity per female of *B. tabaci* MEAM1adults at different constant temperatures**,** resulting from AFT modeling. For the AFT models, the error distributions used, their scales, δ, and the models goodness-of-fit evaluated based upon likelihood ratio test are presented in the lower part of the table.

763 **Table 5.** Estimated parameters of the non-linear models fitted to describe the relationship
764 between temperature and adult senescence rates, oviposition time^{-1}, and average
765 fecundity per females for *B. tabaci* MEAM1.

766 **Table 6.** Comparison of simulated and observed life history parameters of *B. tabaci*
767 MEAM1obtained from the three life tables established in La Molina.

768

769 **Fig. 1.** The relationship between temperature and median development rates for immature life
770 stages of B. *tabaci* MEAM1 (A: eggs, B: nymph, C: puparium). The models (Janisch
771 model (Janisch (1932); see equation in Tab.2), were fitted in terms of *ln*-development
772 time. Broken lines represent 95% confidence limits for the fitted model. Markers are
773 observed median development rates. Bars represent 95% confidence limits of observed
774 data points.

775 **Fig. 2.** Temperature-dependent mortality ratios of *B. tabaci* MEAM1 immature life stages (A:
776 eggs, B: nymph, C: puparium); dots: observed data; bold line: nonlinear model fitted to
777 the data; dashed lines: upper and lower 95% confidence limits of the model.

778 **Fig. 3.** Fecundity of *B. tabaci* MEAM1 and its dependence on temperature and female age; (A)
779 temperature-dependent inverse oviposition time (day^{-1}) of *B. tabaci* MEAM1 females,
780 (B) cumulative proportion of reproduction in relation to normalized female age, (C)
781 total fecundity per female, and (D) female ratios in emerging adults. In A) and C) dots
782 are observed data; solid lines are fitted models (exponential model in A and a parabolic
783 model in C; see Table 5); and broken lines are 95% confidence limits for the fitted
784 model. In B) colored dots are observed data (accumulated mean reproduction/total

785 reproduction per female) at indicated experimental temperatures; bold line is the
786 Weibull distribution model fitted to oviposition data.

787 **Fig. 4.** Comparison of results obtained from three life tables for *B. tabaci* MEAM1 in La
788 Molina with outputs of five stochastically simulated life tables. A) Age-stage specific
789 survival rates (A1: spring, A2: winter, A3 summer); dots are observed data of indicated
790 life stages, lines are stochastic simulation outputs (full line: average of four life table
791 simulations; scattered lines: minimum and maximum values obtained from the four
792 simulations). B) Age-specific survival rates (observed: brown lines, simulated average:
793 grey line, simulated maximum and minimum: scattered grey lines) (B1: spring, B2:
794 winter, B3 summer), and C) age-specific fecundity (observed: brown lines, simulated
795 average: grey line, simulated maximum and minimum: scattered grey lines) (C1:
796 spring, C2: winter, C3 summer).

797 **Fig. 5.** Life table parameters of *B. tabaci* MEAM1 simulated using the phenolgy rate model
798 developed in this study over a temperature range from 0 to 40°C. (A) intrinsic rate of
799 natural increase (r_m), (B) net reproduction rate (R_0) [females/female], (C) finite rate of
800 increase (λ), (D) mean generation time (T) [days], (E) Immature stages survival rate,
801 (S) doubling time (Dt) [days]. Black line: adjusted model prediction if temperature is
802 held constant; scattered black line: adjusted model prediction if temperature fluctuates
803 ±5°C (x-value ±5°C); grey line: original model prediction at constant temperatures.

804 **Fig. 6.** Life history (autecological) parameters of *B. tabaci* MEAM1 reported in the literature
805 plotted against temperature together with the observed data and model predictions of
806 this study; symbols: literature data as indicated in the legend; lines: model predictions.

807 A: egg development rate (literature data on development times were transformed into
808 rates), B: overall inverse development time from egg to adults, C: egg mortality rates,
809 D: overall survival rates from egg to adult emergence, E: female senescence rates, F:
810 fecundity per female, and G: finite rate of population increase, λ.

811

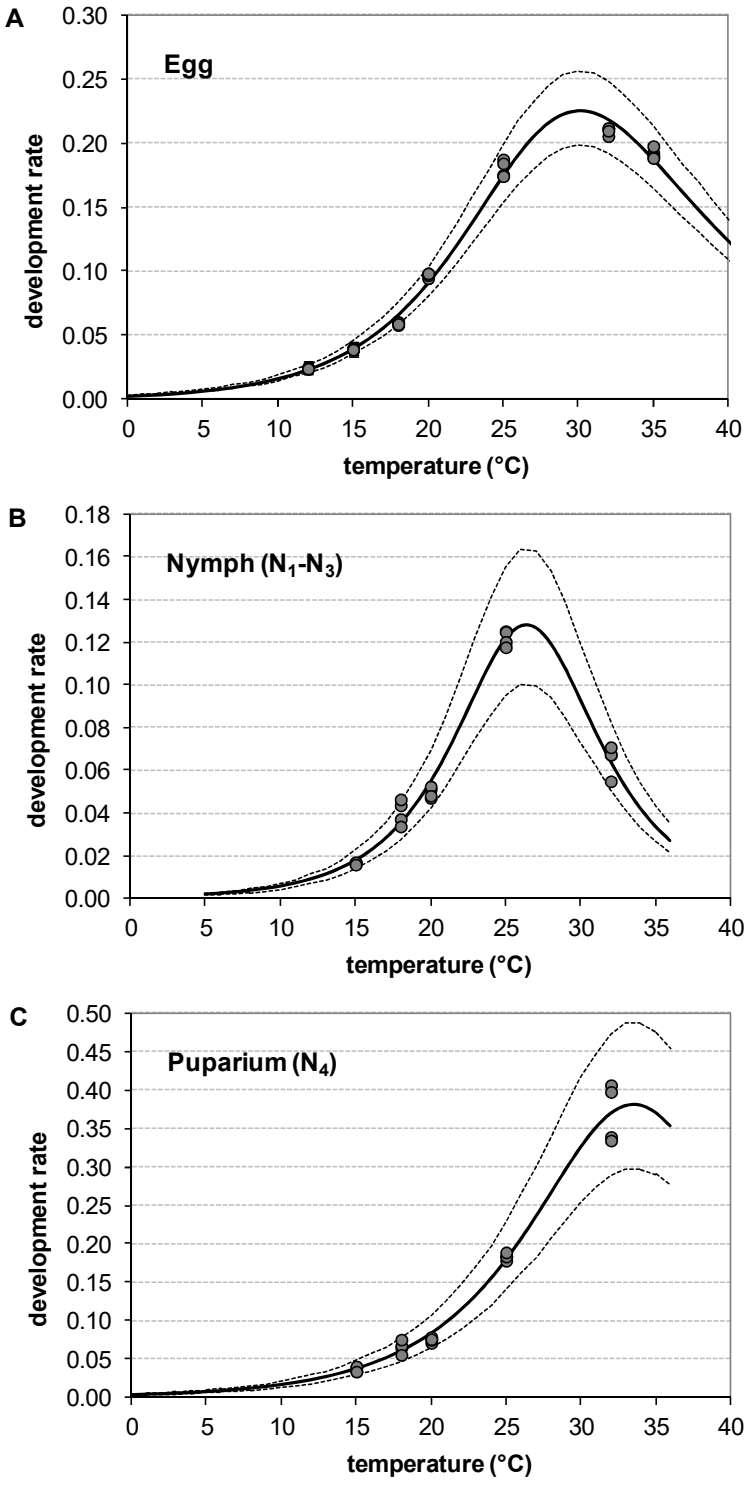

Fig. 1. The relationship between temperature and median development rates for immature life stages of B. *tabaci* MEAM1 (A: eggs, B: nymph, C: puparium). The models (Janisch model (Janisch, 1932); see equation in Tab.2) were fitted in terms of *ln*-development time. Broken lines represent 95% confidence limits for the fitted model. Markers are observed median development rates.

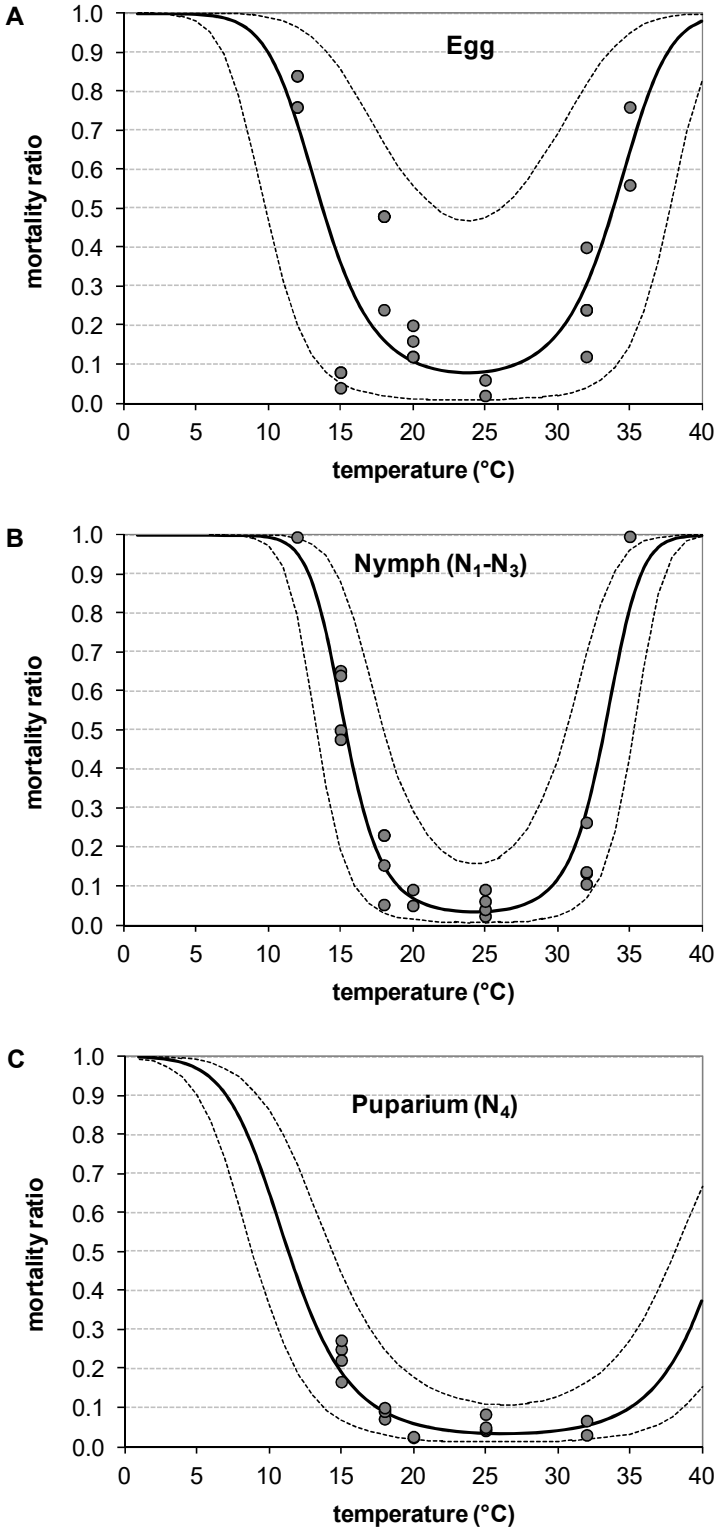

Fig. 2. Temperature-dependent mortality ratios of *B. tabaci* MEAM1 immature life stages (A: eggs, B: nymph, C: puparium); dots: observed data; bold line: nonlinear models fitted; dashed lines: upper and lower 95% confidence limits of the model.

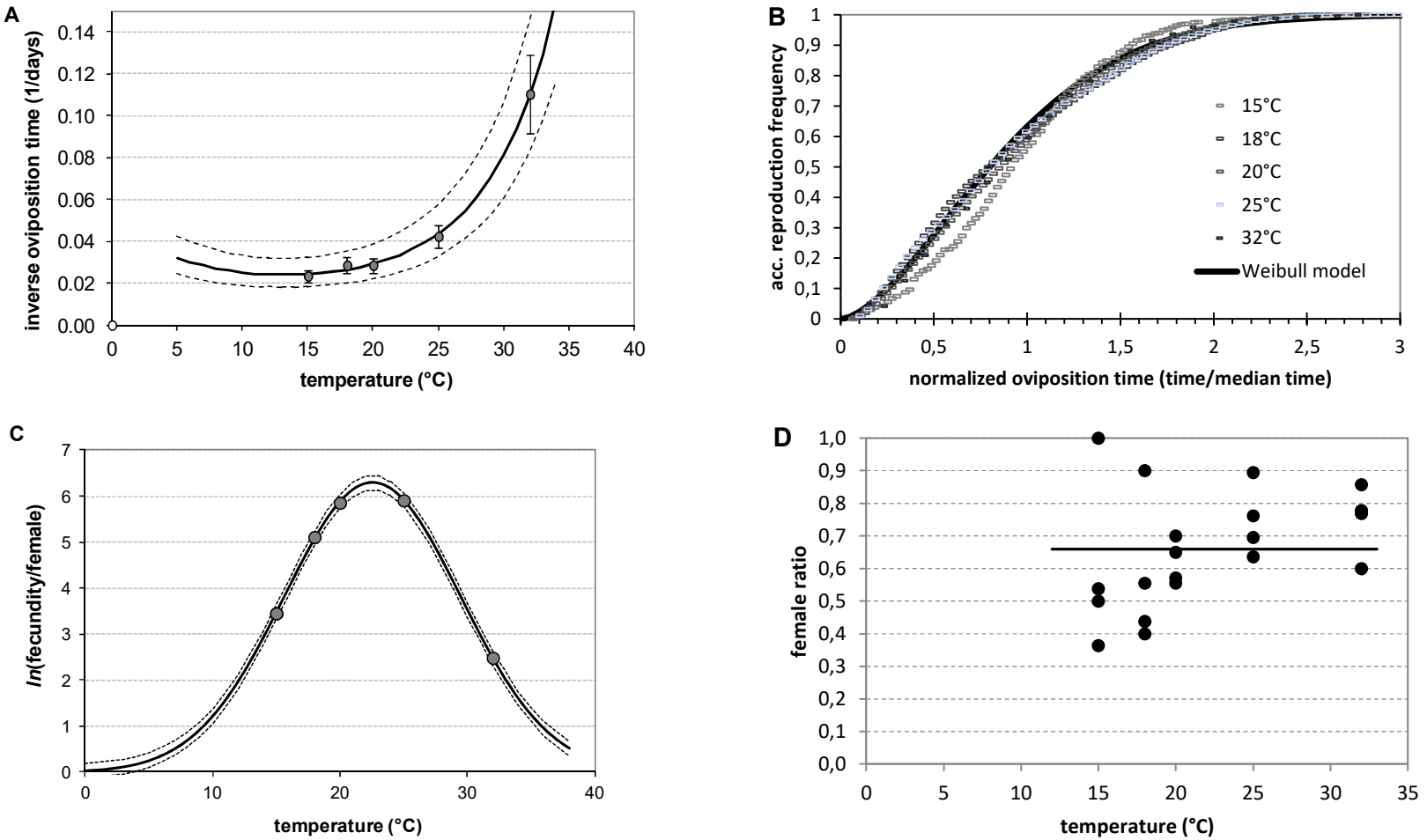

Fig. 3. Fecundity of B. tabaci MEAM1 and its dependence on temperature and female age; (A) temperature-dependent inverse oviposition time (day-1) of B. tabaci MEAM1 females, (B) cumulative proportion of reproduction in relation to normalized female age, (C) total fecundity per female, and (D) female ratios in emerging adults. In A) and C) dots are observed data; solid lines are fitted models (exponential model in A and a parabolic model in C; see Table 5); and broken lines are 95% confidence limits for the fitted model. In B) colored dots are observed data (accumulated mean reproduction/total reproduction per female) at indicated experimental temperatures; bold line is the Weibull distribution model fitted to oviposition data.

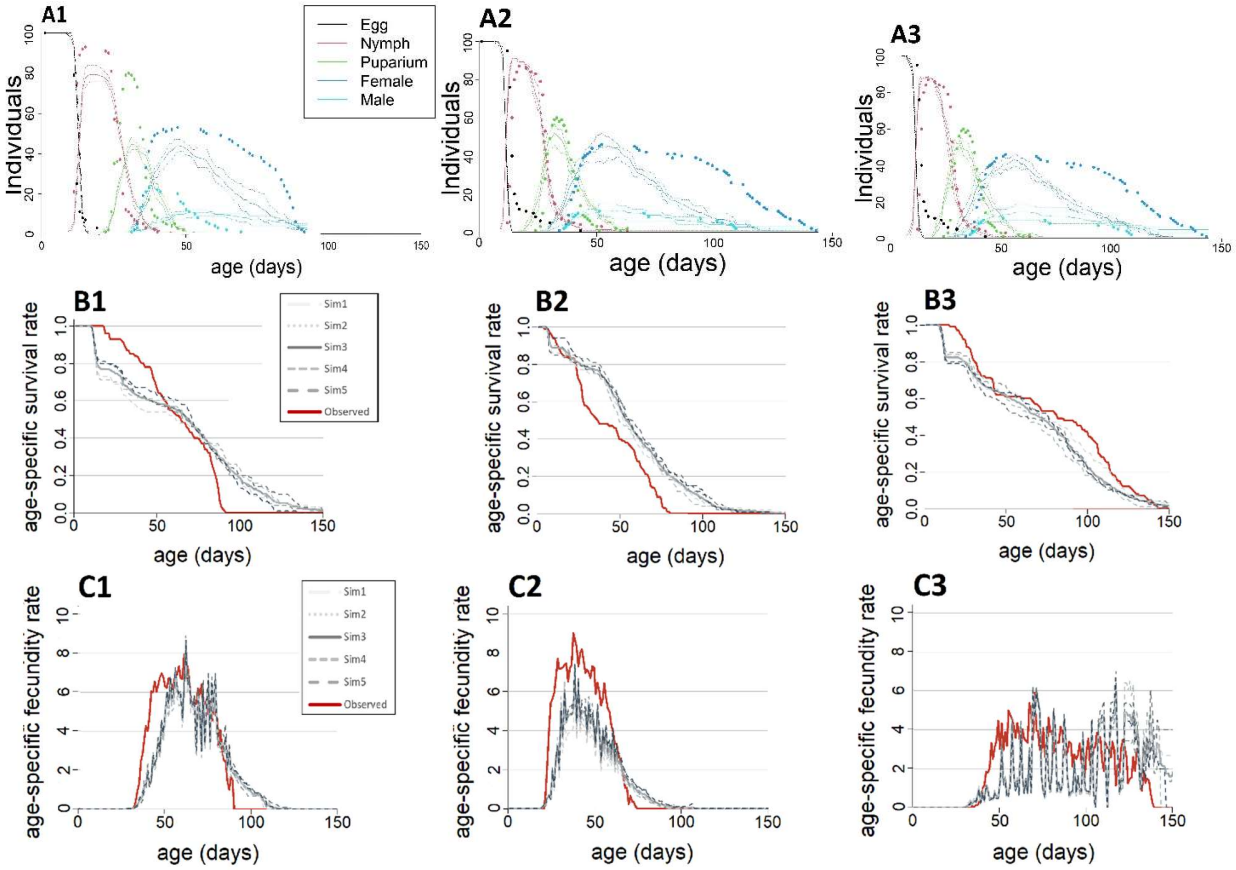

Fig. 4. Comparison of results obtained from three life-tables for *B. tabaci* MEAM1 in La Molina with outputs of five stochastically simulated life tables. A) Age-stage specific survival rates (A1: spring, A2: winter, A3 summer); dots are observed data of indicated life stages, lines are stochastic simulation outputs (full line: average of four life table simulations; scattered lines: minimum and maximum values obtained from the four simulations). B) Age-specific survival rates (observed: red lines, simulated average: grey line, simulated maximum and minimum: scattered grey lines) (B1: spring, B2: winter, B3 summer), and C) age-specific fecundity (observed: red lines, simulated average: grey line, simulated maximum and minimum: scattered grey lines) (C1: spring, C2: summer, C3: winter).

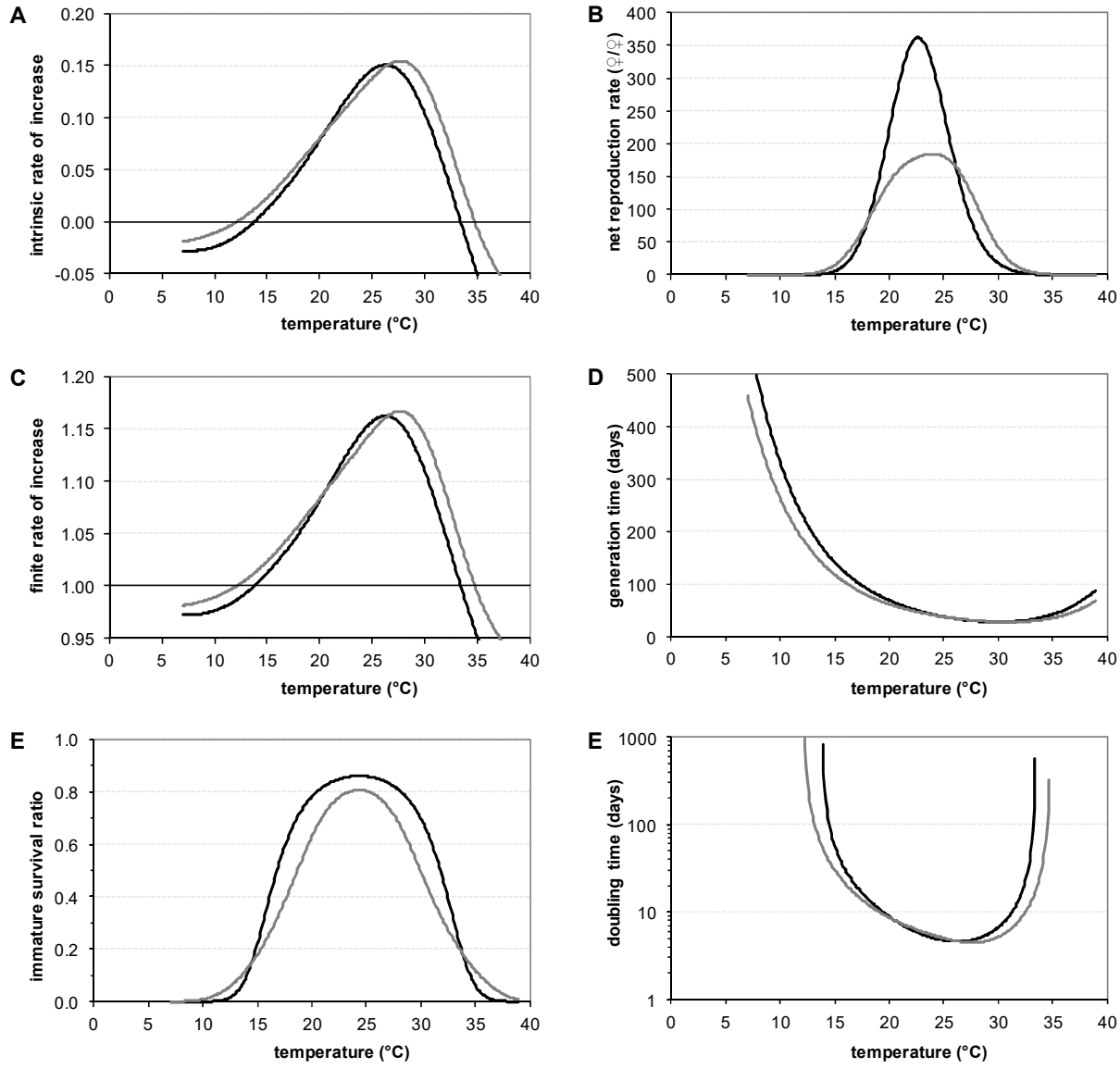

Fig. 5. Life table parameters of *B. tabaci* MEAM1 simulated using the phenolgy rate model developed in this study over a temperature range from 0 to 40°C. (A) intrinsic rate of natural increase (r_m), (B) net reproduction rate (R_0) [females/female], (C) finite rate of increase (λ), (D) mean generation time (T) [days], (E) Immature stages survival rate, (*S*) doubling time (*Dt*) [days]. Black line: adjusted model prediction if temperature is held constant; scattered black line: adjusted model prediction if temperature fluctuates ±5°C (x-value ±5°C); grey line: original model prediction at constant temperatures.

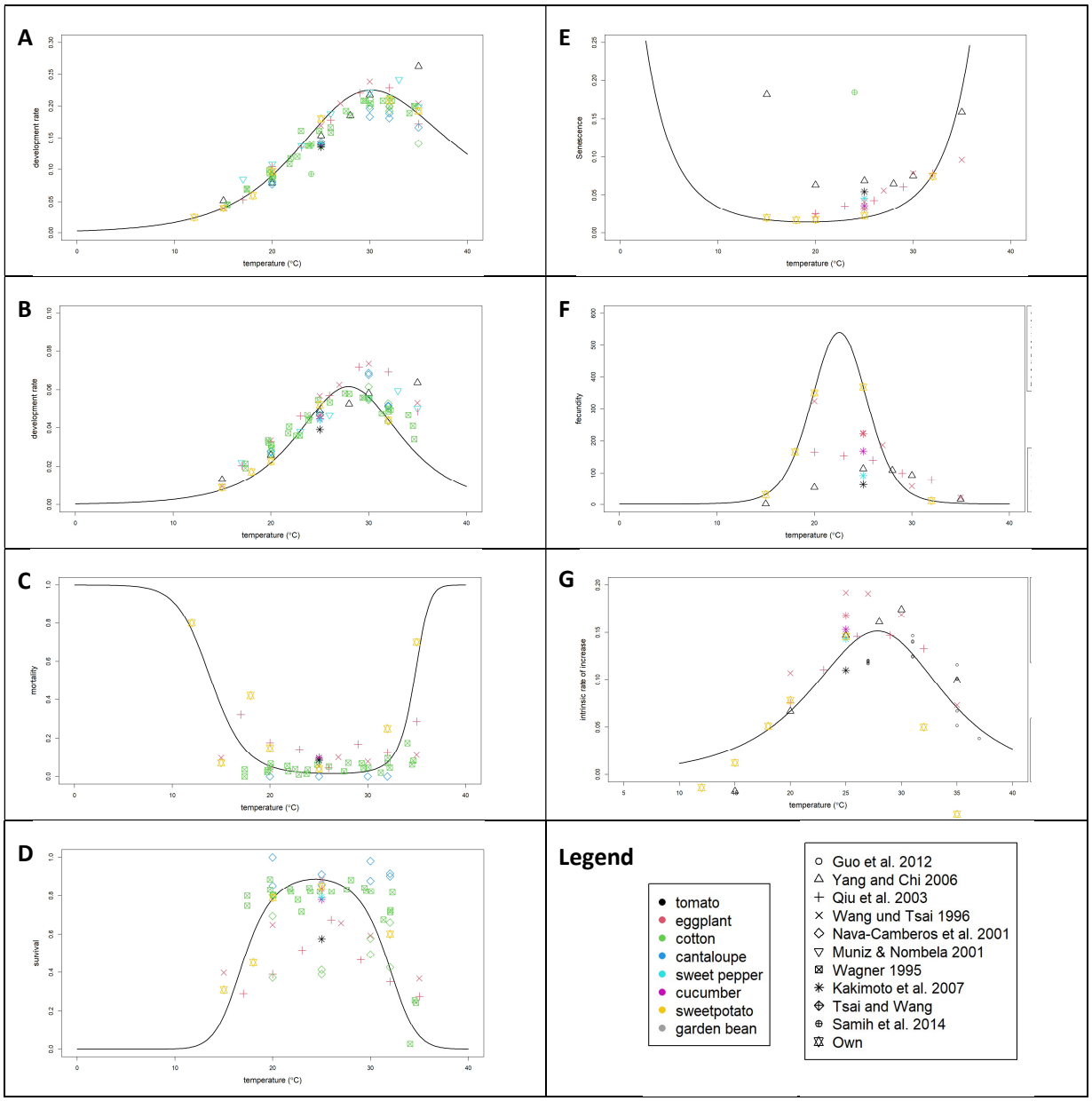

Fig. 6. Life history (autecological) parameters of *B. tabaci* MEAM1 reported in the literature plotted against temperature together with the observed data and model predictions of this study; symbols: literature data as indicated in the legend; lines: model predictions. A: egg development rate (literature data on development times were transformed into rates), B: overall inverse development time from egg to adults, C: egg mortality rates, D: overall survival rates from egg to adult emergence, E: female senescence rates, F: fecundity per female, and G: finite rate of population increase, λ.

Table 1. Median development times resulting from accelerated failure time modeling and observed survival rates in the immature *B. tabaci* MEAM1 life-stages at constant temperatures. For the AFT models, the error distributions used, their scales, δ, and the models goodness-of-fit evaluated based upon likelihood ratio test are presented in the lower part of the table.

Temp.		Eggs		Nymphs		Puparia	
	N [A]	Median dev. time	Survival	Median dev. time	Survival	Median dev. time	Survival
(°C)		(days) [B]	(%)[D]	(days)	(%)	(days)	(%)
12	100	41.1 (38.6-43.7)a	20 (±9.4)	-	0	n.a.	n.a.
15	100	25.5 (23.8-27.3)b	93 (±5.9)	60.1 (52.5-68.9)a	43 (±11.5)	25.9 (21.2-31.6)a	77.5 (±15.3)
18	100	16.8 (15.6-18.1)c	58 (±10.9)	25.8 (21-31.6)b	84.5 (±10.9)	15.1 (11.8-19.2)b	91.8 (±9.2)
20	100	10.3 (9.6-11.1)d	85 (±7.9)	20.2 (17.1-23.9)c	95.3 (±5.4)	13.3 (10.7-16.6)b	97.5 (±4.2)
25	100	5.6 (5.2-6)e	96 (±4.5)	8.2 (6.9-9.6)d	93.8 (±5.6)	5.4 (4.4-6.8)c	94.4 (±5.5)
32	100	4.8 (4.4-5.1)f	75 (±9.4)	15.3 (12.6-18.5)c	14 (±3.4)	2.8 (2.2-3.5)d	95.2 (±6.3)
35	100	5.2 (4.8-5.7)ef	30 (±9.8)	-	0	n.a.	n.a.
	Error Dist.[C]	log-logistic		log-logistic		log-logistic	
	Scale δ	0.0519 (±0.0023)***		0.1563 (±0.0073)***		0.1333 (±0.0068)***	
		Likelihood ratio test		Likelihood ratio test		Likelihood ratio test	
Model		*ln* L	ΔDeviance	*ln* L	ΔDeviance	*ln* L	ΔDeviance
Null(Intercept only)		-1586.2	2072.9	-1267.7	1180.9	-999.9	1370.4
(1) λ each temperature		-670.7	241.9	-976.6	598.7	-645.1	660.8
(2) λ for each batch		-662.1	224.7	-968.0	581.5	-635.8	642.2
Saturated model		-549.7		-677.3	-	-314.7	-
F: (1) against Null		$F(df_x,df_{x-1})$ = 151.4 (P<0.001)		$F(df_x,df_{x-1})$ = 45.7 (P<0.001)		$F(df_x,df_{x-1})$ = 30.6 (P=0.002)	
F: (2) against (1)		$F(df_{x-1},df_{x-2})$ = 0.4 (P=0.999)		$F(df_{x-1},df_{x-2})$ = 0.3 (P>0.999)		$F(df_{x-1},df_{x-2})$ = 0.2 (P>0.999)	

	df		*df*		*df*
Null(Intercept only)	126	-1267.7	192	-999.9	118
(1) λ each temperature	120	-976.6	188	-645.1	114
(2) λ for each batch	99	-968.0	173	-635.8	99
Saturated model	(n=128)	-677.3	(n=194)	-314.7	(n=120)

[A] N is the initial number of individuals used; surviving individuals from each life-stage were used in the evaluation of the subsequent life-stage. Total number of individuals tested were n =457 (eggs), n =323 (nymphs), and n =300 (puparia).

[B] Numbers in parenthesis are 95% confidence limits based on t-distribution (a heterogeneity factor, H = deviance/df, was included to calculate the limits). Medians followed by different letters in the same columns are significantly different (P < 0.05) according to the AFT model.

[C] δ is the scale of the selected distribution link function; the figures in () are SE of δ ("***" indicates P < 0.001). The accumulated development frequency (AccDevFreq) in relation to normalized age (time/median time) is calculated according to the selected distribution link function; for the log-logistic link function: AccDevFreq(x) = 1-(1/(1+x^{α})), where x is the normalized age (determined through rate summation), and $\alpha = 1/\delta$.

[D] Numbers in parenthesis are SE calculated using the formula: SE = sqrt([m*{1-m}]/N), where m is the mortality rate and N is the number of test insects.

Table 2. Estimated parameters of the Janisch model fitted to describe temperature-dependent median development rates (1/day) in immature life-stages of *B. tabaci* MEAM1.

Life stages	Parameter estimates of the Janisch (1932) model[A]				*F*-value	$df_{1, 2}$	*P*	r^2_{adj}
	D_{min}	T_{opt}	k_1	k_2				
Egg	4.615 (±0.275)***	28.2 (±0.86)***	0.103 (±0.024)***	0.18 (±0.007)***	1474.7	3, 24	<0.001	0.994
Nymph (N_1-N_3)	7.791 (±0.403)***	26.5 (±0.18)***	0.235 (±0.008)***	= k_1	306.1	2, 17	<0.001	0.97
Puparium (N_4)	2.62 (±0.217)***	33.6 (±1.13)***	0.162 (±0.008)***	= k_1	610.5	2, 17	<0.001	0.985

Numbers in parenthesis are standard errors. Parameter values significantly different from zero are indicated by asterisks (P < 0.05 = *, P < 0.01 = **, P < 0.001 = ***). [A] The equation of the Janisch model (Janisch 1932) is:

$$\boldsymbol{r(T) = \left\{\frac{D_{min}}{2}(exp\,(k_1[T - T_{opt}]) + exp\,(-k_2[T - T_{opt}]))\right\}^{-1}}$$

where $r(T)$ is the development rate at temperature T, T_{opt} the temperature at which the development rate is at maximum, D_{min} the development time (in days) at T_{opt}, and k_1 and k_2 are fitted constants (if $k_1 = k_2$ the curve has a symmetrical shape).

Tab. 3. Estimated parameters of the nonlinear model fitted to describe temperature-dependent mortality in immature life stages of B. tabaci MEAM1

Life Stages	Parameter estimates of the model[A]			*F* value	$df_{1,2}$	*P*	Adj. R^2
	T_{opt}	m_{min}	α_i				
Egg	23.8 (±1.27)***	0.078 (±0.083)^{ns}	0.0245 (±0.0131)^{ns}	13.76	22, 24	<0.001	0.556
Nymph	24.3 (±0.26)***	0.032 (±0.012)**	0.0426 (±0.0058)***	43.76	17, 19	<0.001	0.818
Puparium	26.2 (±3.25)***	0.035 (±0.022)^{ns}	0.015 (±0.0126)^{ns}	12.5	12, 14	<0.001	0.622

[A] The models fitted was eq. 7 described in the text.

[B] Numbers in parenthesis are standard errors. Parameter values significantly different from zero are indicated by asterisks (P < 0.05 = *, P < 0.01 = **, P < 0.001 = ***).

Table 1. Female survival times, oviposition times (resulting from accelerated failure time modeling) and total fecundity per female of *B. tabaci* MEAM1 adults at different constant temperatures. For the AFT models, the error distributions used, their scales, δ, and the models goodness-of-fit evaluated based upon likelihood ratio test are presented in the lower part of the table.

Temp. (°C)	N [A] (f / m)	Female survival time T_{63}±STD (days) [B]	Oviposition time T_{63}±STD (days)	Fecundity per female (Mean±STD)	CL(95%)	max. [C]
15	16/15	60.6 (±11.05)a	46.2 (±1.81)a	31.6 (±28.3)a	(3.8-59.3)	[81.5]
18	25/20	71.7 (±15.98)a	38.1 (±1.58)a	165.9 (±29.7)b	(136.8-195)	[187.6]
20	49/30	68.8 (±13.96)a	37.9 (±1.51)a	350.2 (±19)c	(331.6-368.8)	[374.6]
25	63/22	52.9 (±10.68)a	25.6 (±1.01)b	368.3 (±43.8)c	(325.4-411.2)	[428.2]
32	45/15	16 (±3.41)b	10.1 (±0.54)c	12 (±2.5)a	(9.6-14.4)	[14.2]
	Model [D]	Weibull	Weibull			
	λ_{male} [E] =	-0.131 (±0.0609)				
	scale δ	0.4907 (±0.0241)***	0.7741 (±0.0207)***			

	ln L	ΔDeviance	*df*	*ln* L	ΔDeviance	*df*	ANOVA [F]	
Intercept only	-1421.3	982.7	218	-188520.8	8570.8	225	$F_{(4, 15)}$ =	143.8
(1) Temp.+λ_{male}	-1330.9	801.9	213	-185734.8	2998.8	220		(P<0.001)
(2) Temp.*Sex	-1330.7	801.5	209					
Saturated model	-930.0		(n=220)	-184235.4		(n=227)		
F: (1) against Null	$F_{(5, 218)}$ = 9.6 (P=0.009)			$F_{(5, 225)}$ = 81.8 (P=<0.001)				
F: (2) against (1)	$F_{(4, 213)}$ = 0.026 (*P*>0.999)							

[A] *N* is the number of females (f) and male (m) adult individuals evaluated at each temperature. Total number of oviposited eggs was *n* =45,558.

[B] Figures are for females. Numbers in parenthesis are 95% confidence limits (due to overdispersion a heterogeneity factor, *h* = *deviance*/*df*, was included to calculate the limits). $T_{63\%}$-values followed by different letters in the same columns are significantly different (P < 0.05) according to the AFT model.

[C] Numbers in [] are maximum numbers of eggs/female observed at each temperature

[D] δ is the scale of the selected distribution link function for survival and oviposition time; the figures in () are SE (values significantly different from zero are indicated by asterisks (P < 0.05 = *, P < 0.01 = **, P < 0.001 = ***). The accumulated senescence and oviposition frequency in relation to normalized age (time/median time) is calculated according to the selected distribution link function; for example, for the Weibull link function: accu. frequency = 1-*exp*(-*exp*[*ln*{$x \times exp(1)$} × α] × *exp*[-α]), where *x* is the normalized age (determined through rate summation), and $\alpha = 1/\delta$.

[E] Adult sex was used as an additive factor in the AFT model; according to the parameter, the lifetime of males was 12,3% (±5.5%) shorter than of females.

[F] ANOVA was performed on *ln*-transformed fecundities (x'= *ln*[x + 1]), where variance between groups were homogeneous (Levene test: P =0.14).

Tab. 5. Estimated parameters of the non-linear models fitted to describe the relationship between temperature and adult senescence rates, oviposition time^{-1}, and average fecundity per females for *B. tabaci* MEAM1.

Response variable	Model	Parameters		*F*-value	$df_{1, 2}$	*P*	adj. R^2
			value (±SE)				
Female senescence rate	remodeled	lnD_{max}	4.265 (±0.02)***	1279.8	2, 9	>0.001	0.9965
	quadratic	T_p	19.209 (±0.302)***				
		α	-0.0091 (±0.0005)***				
Oviposition time^{-1}	remodeled	lnD_{max}	3.73 (±0.088)***	178	2, 4	0.006	0.9889
	quadratic	T_p	13.245 (±2.492)*				
		α	-0.004 (±0.001)*				
Fecundity per female	Taylor	lnF_{max}	6.293 (±0.039)***	3612.5	2, 4	>0.001	0.9994
		T_{opt}	22.551 (±0.048)***				
		T_δ	-6.926 (±0.051)***				

Numbers in parenthesis are standard errors. Parameter values significantly different from zero are indicated by asterisks (P < 0.05 = *, P < 0.01 = **, P < 0.001 = ***). The models are shown in the text: Taylor model (eq. 4), remodeled quadratic (eq.5).

The remodeled quadratic model is:

$$ln\left(D(T_i)\right) = ln\left(\frac{1}{r(T_i)}\right) = lnD_{max} + \alpha(T_p - T_i)^2$$

where $D(T_i)$ is the senescence/oviposition time and $r(T_i)$ the senescence rate/inverse oviposition time at temperature T_i, T_p the temperature at which the senescence/oviposition time is at maximum, lnD_{max} is the ln senescence/oviposition time at T_p and α is a shape parameter; and the Taylor model is:

$$ln\left(F(T_i)\right) = ln\left(\frac{1}{r(T_i)}\right) = lnF_{max} \times exp\left(-\frac{1}{2}\left[\frac{T - T_{opt}}{T_\delta}\right]^2\right)$$

where $F(T_i)$ is the fecundity per female at temperature T_i, T_{opt} the temperature at which fecundity is at maximum, lnF_{max} is the ln maximum fecundity at temperature T_{opt}, and T_δ is a shape parameter.

Table 6. Comparison of simulated and observed life history parameters of *B. tabaci* MEAM1 obtained for the three life tables established in La Molina during different seasons. Each life table consisted of *n*=100 individuals.

	Spring 2011			Winter 2011			Summer 2012		
Avg. daily temp. cycle	16.4 (±2)°C-26.4(±3)°C			14.6 (±1.4)°C-21.3(±4.2)°C			19.5 (±1.2)°C-29.7(±2.4)°C		
	Sim.[B] (±STD)	Obs.	P[A]	Sim (±STD)	Obs.	P[A]	Sim (±STD)	Obs.	P[A]
Life-table parameters									
r_m	0.08 (±0.002)	0.1	<0.001	0.069 (±0.002)	0.078	<0.001	0.124 (±0.002)	0.144	<0.001
R_0	100.5 (±8.8)	155.3	<0.001	71.2 (±9.4)	129.9	<0.001	106.3 (±13.6)	129.3	0.090
GRR	238.8 (±19.1)	285.4	0.015	285.7 (±53.2)	293.1	0.889	183.6 (±21.8)	274.2	<0.001
T	57.75 (±0.65)	50.39	<0.001	62.04 (±1.31)	62.33	0.821	37.45 (±0.68)	33.84	<0.001
λ	1.083 (±0.002)	1.105	<0.001	1.071 (±0.002)	1.081	<0.001	1.133 (±0.002)	1.155	<0.001
Dt (days)	8.69 (±0.23)	6.92	<0.001	10.1 (±0.28)	8.88	<0.001	5.57 (±0.1)	4.82	<0.001
Development time (days)									
Egg	12.94 (±0.11)	11.02	<0.001	11.62 (±0.11)	13.09	<0.001	7.76 (±0.03)	6.92	<0.001
Nymph	16.12 (±0.44)	15.41	0.107	16.25 (±0.39)	16.58	0.389	11.68 (±0.22)	8.61	<0.001
Pupa	10.09 (±0.25)	9.31	0.002	12.65 (±0.42)	12.42	0.592	6 (±0.26)	6.4	0.120
Total (Egg-Adult)	39.15 (±0.54)	35.74	<0.001	40.51 (±0.49)	42.1	0.001	25.45 (±0.33)	21.93	<0.001
Mortality rate									
Egg	0.26 (±0.063)	0.07	0.003	0.174 (±0.037)	0.13	0.236	0.13 (±0.038)	0.06	0.066
Nymph	0.21 (±0.067)	0.022	0.005	0.14 (±0.032)	0.207	0.034	0.085 (±0.031)	0.106	0.483
Pupa	0.08 (±0.055)	0.11	0.584	0.065 (±0.051)	0.145	0.119	0.045 (±0.019)	0.048	0.874
Total (Egg-Adult)	0.464 (±0.054)	0.190	<0.001	0.336 (±0.046)	0.41	0.105	0.239 (±0.024)	0.2	0.102
Adult survival and fecundity									
Females (N_f)	35.4 (±2.5)	55	<0.001	53.6 (±3.9)	48	0.152	38.8 (±5.5)	38	0.884
Female ratio (N_f/N_A)	0.663 (±0.049)	0.68	0.745	0.808 (±0.050)	0.81	0.908	0.51 (±0.062)	0.48	0.574
F surv. time (days)	48.6 (±4.22)	42.1	0.126	51.2 (±3.73)	68	<0.001	43.8 (±2.9)	40.4	0.243
Oviposition time (days)	24.1 (±0.28)	21.2	<0.001	35.8 (±3.05)	34.1	0.570	18 (±0.48)	18.8	0.082
Fecundity/female	283.7 (±12.72)	282.3	0.910	132.5 (±10.74)	276.3	<0.001	274.9 (±14.79)	340.4	<0.001
eggs/female/day	5.9 (±0.32)	6.7	0.008	2.6 (±0.03)	4	<0.001	6.3 (±0.27)	8.4	<0.001

[A] P-values revealing significant differences between observed and simulated values ($P < 0.05$) according to z-scores are underlined.

[B] "Sim." is the average (±standard deviation) of five stochastic life table simulations (n=100).